Supplementary Information

Microfluidic-Driven Ultrafast Self-assembly of Dipeptide into Stimuli-responsive 0D, 1D, and 2D Nanostructures and as Hydrolase Mimic

Ashmeet Singh‡, Jeong-Un Joo‡, Dong-Pyo Kim*

Affiliations & Address

Center for Intelligent Microprocess of Pharmaceutical Synthesis (CIMPS), Department of Chemical Engineering, Pohang University of Science and Technology (POSTECH), Pohang, South Korea, 37673.

‡Authors contributed equally to this work.

*Corresponding author: Dong-Pyo Kim (e-mail: dpkim@postech.ac.kr)

Table of Contents

1. Materials & Methods:

HPLC water, sodium hydroixde (NaOH), zinc nitrate, tetrabutylammonium iodide (TBAI) and 5,5-dithio-bis-(2-nitrobenzoic acid) (DTNB) were purchased from Sigma Aldrich. 1,1,1,3,3,3-Hexafluoro-2-propanol (HFIP) was purchased from TCI Co. Ltd. Hydrogen peroxide (H_2O_2, 34.5%) was purchased from Samchun Pure Chemical Co. Ltd. All capillary reactors, Polytetrafluoroethylene (PTFE, inner diameter 300 μm and 500 um) tubing, Polyetherketone (PEEK, inner diameter 500 μm) T-junctions and 4-port Manual Switching Valve (PEEK, rotary valve, 1 mm inner diameter) were purchased from IDEX HEALTH & SCIENCE (WA, USA). PHD Ultra and Legato 200, syringe pumps, were purchased from Harvard Apparatus and KD Scientific respectively.

2. Characterization of Dipeptide Amphiphile:

A modified dipeptide **Fmoc-CH** (N-terminal; Fmoc- and C-terminal; Acid) was purchased from Genscript. The dipeptide was purified by RP-HPLC using an Inertsil ODS-3 4.6 x 250 mm column with acetonitrile (ACN) and water (H_2O) as mobile phase solvents containing 0.065% and 0.05% TFA (v/v) respectively. Pure dried peptides were obtained after evaporation of Acetonitrile (ACN) and subsequent lyophilzation.

HPLC:

Pump A: 0.065% TFA in 100% H_2O (v/v) Pump B: 0.05% TFA in 100% ACN (v/v)

Total Flow Rate: 1 mL/min, Detector Wavelength: 220 nm

Time Module Command Value

Table S1: Gradient flow with time during HPLC run.

Time	Pump A (%)	Pump B (%)
0.01	80	20
25	20	80
25.01	5	95
27.00	5	95
27.01	80	20
35.00	80	20
35.01	Controller Stop	

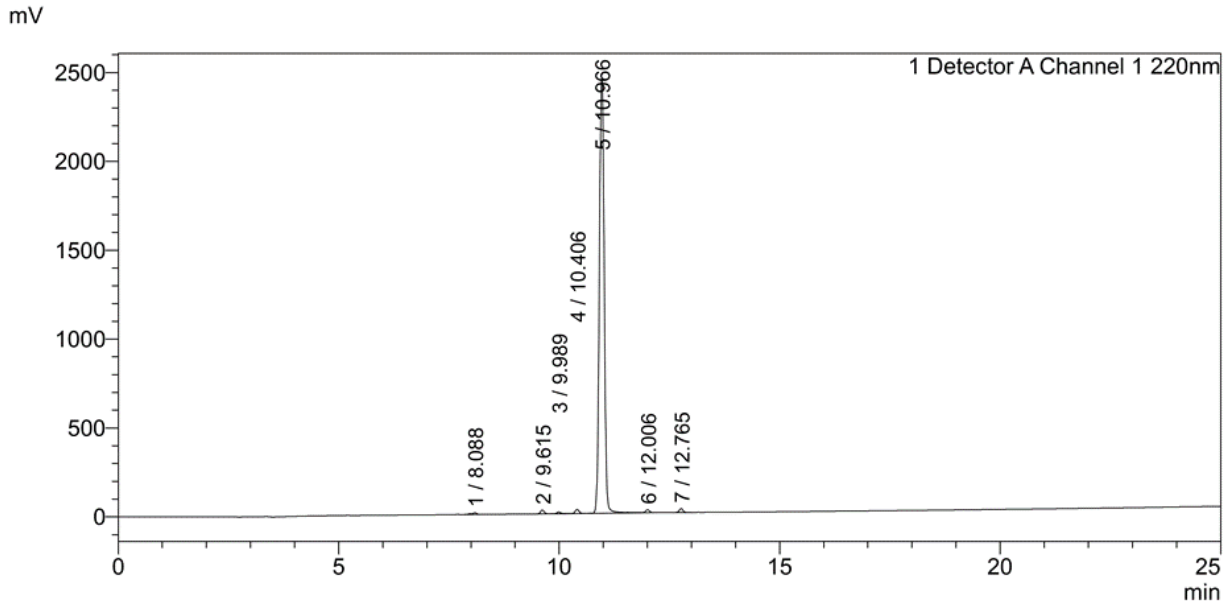

Fig. S1. HPLC chromatogram shows the purity of the peptide which was eluted at a retention time of 10.96 min that corresponds to 46.32% of ACN and 53.68% of H_2O.

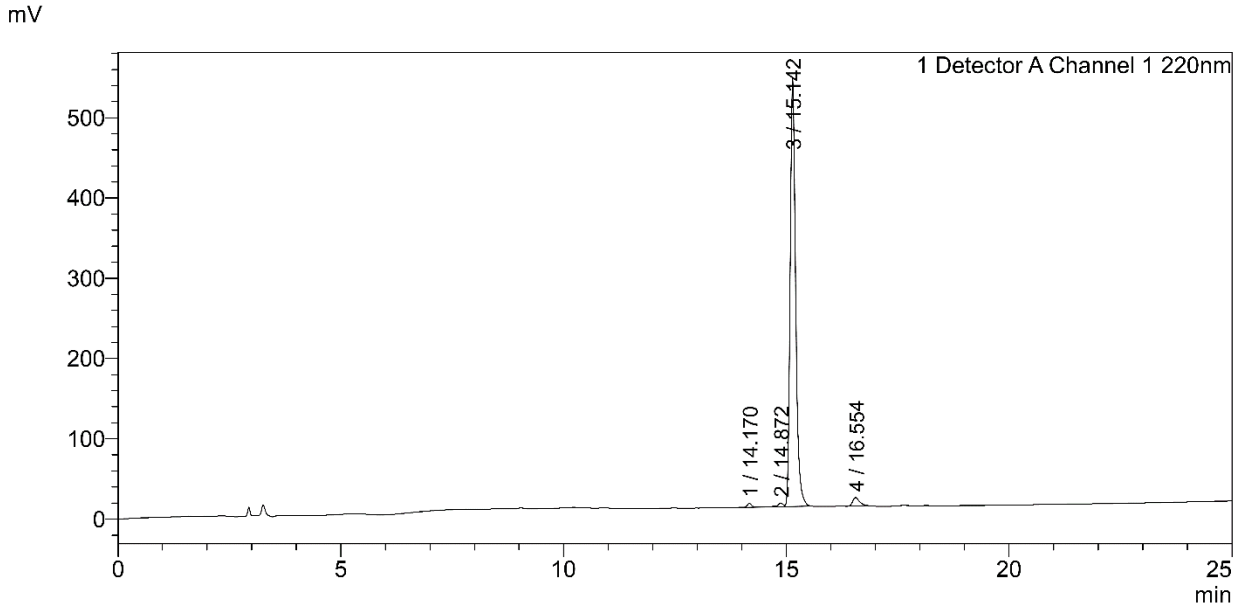

Fig. S2. HPLC chromatogram of the oxidized peptide that showed the purity of the peptide with an increased in the retention time of 15.14 min that corresponds to 56.34% of ACN and 43.66% of H_2O.

Mass Spectrometry:

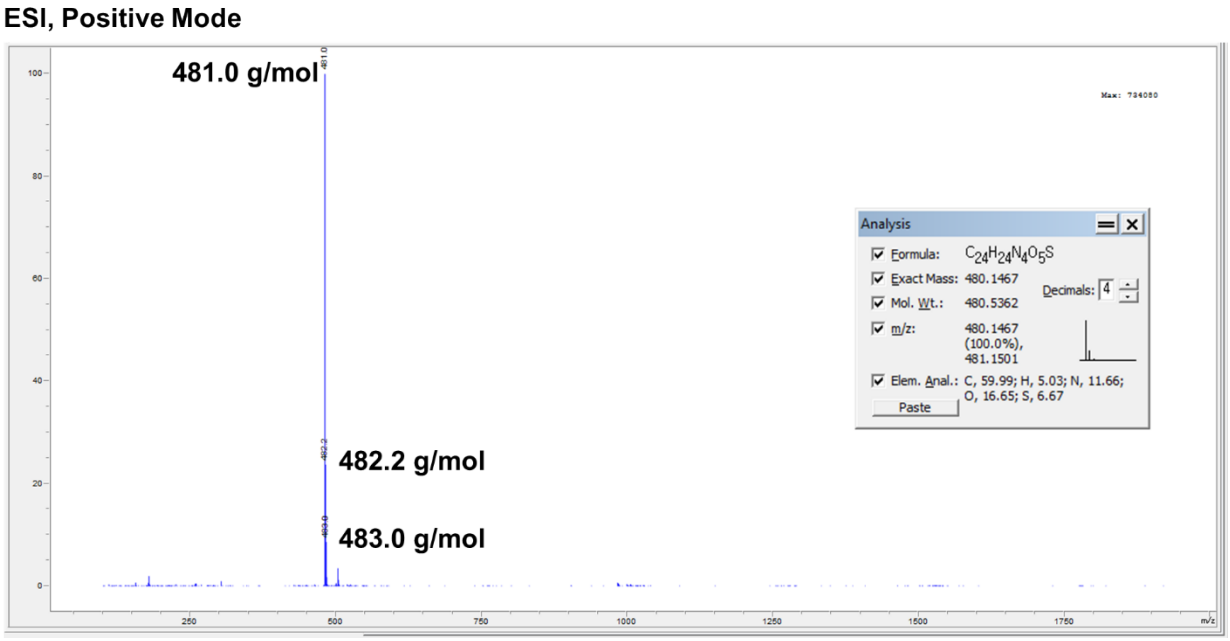

Fig. S3. Mass spectrum was recorded to confirm the molecular weight. The calculated m/z for ***1*** ($C_{24}H_{24}N_4O_5S$) was 480.14 g/mol and mass found was 481.0 g/mol $[M+H]^+$.

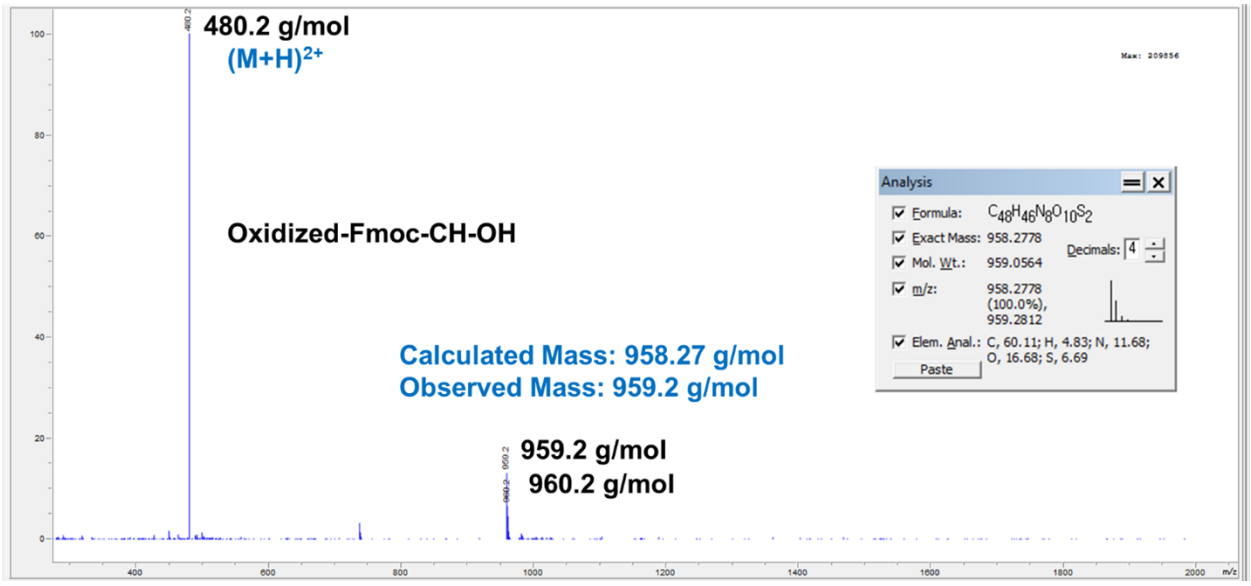

Fig. S4. Positive mode mass spectrum of the oxidized peptide (**ox-1**) to confirm the molecular weight. The calculated m/z for ***1*** ($C_{48}H_{46}N_8O_{10}S_2$) was 958.27 g/mol and mass found was 959.2 g/mol $[M+H]^+$. The $[M+H]^+$ showed the highest intensity as a result of m/z value where z=2.

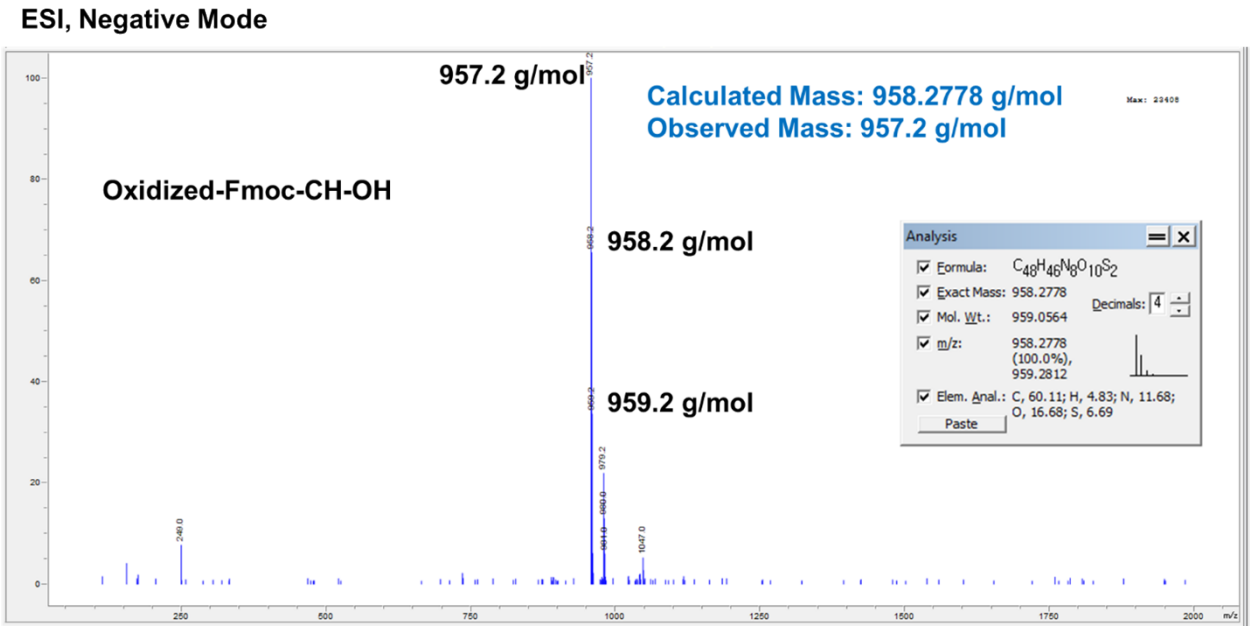

Fig. S5. Negative mode mass spectrum of the oxidized peptide to confirm the molecular weight. The calculated m/z for ***1*** **(**$C_{48}H_{46}N_8O_{10}S_2$) was 958.27 g/mol and mass found was 957.2 g/mol. The negative mode showed the highest intensity at 957.2 g/mol.

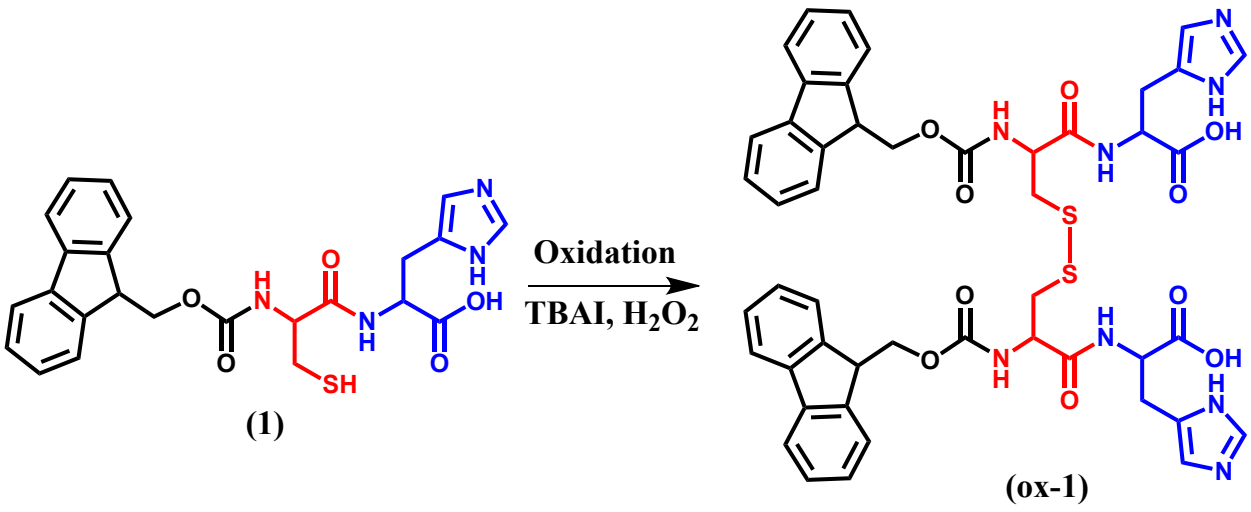

Fig. S6. Chemical structural change before (left) and after (right) oxidation.

Entry	Final conc. of 1 (mM)	Flow rate (µL/min)			PTFE Channel Specification		Residence time (s)	Incubation Time (h)	Self-assembly	
		1 (HFIP)	Water	Total	Diameter (φ, µm)	Length (l, m)			Flow	Batch
1	2	200	1800	2000	500	1.4	8.2	~0	-	-
2								2	NP	NP
3								20	NP	NP
4	2	100	900	1000			16.5	0	-	-
5								2	NP	NP
6								20	NP	NP
7	5	100	900	1000			16.5	~0	-	-
8								2	TB	NP
9								20	TB	TB
10	5	100	900	1000	300		5.94	~0	-	-
11								2	NP	NP
12								20	TB	TB
13	5	10	90	100			59.4	~0	**TB**	-
14								2	TB	NP
15								20	TB	TB

3. Microfluidic Driven Self-assembly Process:

Table S2: Standardization of peptide concentration, channel specifications, and flow rate for **TB** formation.

Table S3: Standardized channel specifications required for the formation of nanostructures.

Self-assembled Nanostructure	Flow rate (µL/min)				Total flow rate (µL/min)	Channel specification		Residence time (s)
						Diameter (φ, µm)	Length (l, m)	
Twisted Bundle (**TB**)	*1* (HFIP)		HPLC water		100	300	1.4	59.4
	10		90					
Nanoparticle (**NP**)	*1* in HFIP		HPLC water + NaOH		106	300	1.4	56
	10		96					
Nanofiber (**NF**)	*1* in HFIP	HPLC water + NaOH	TBAI	H_2O_2	166	300	1.4+2.8	114.1 (43.6+71.5)
	10	96	30	30				

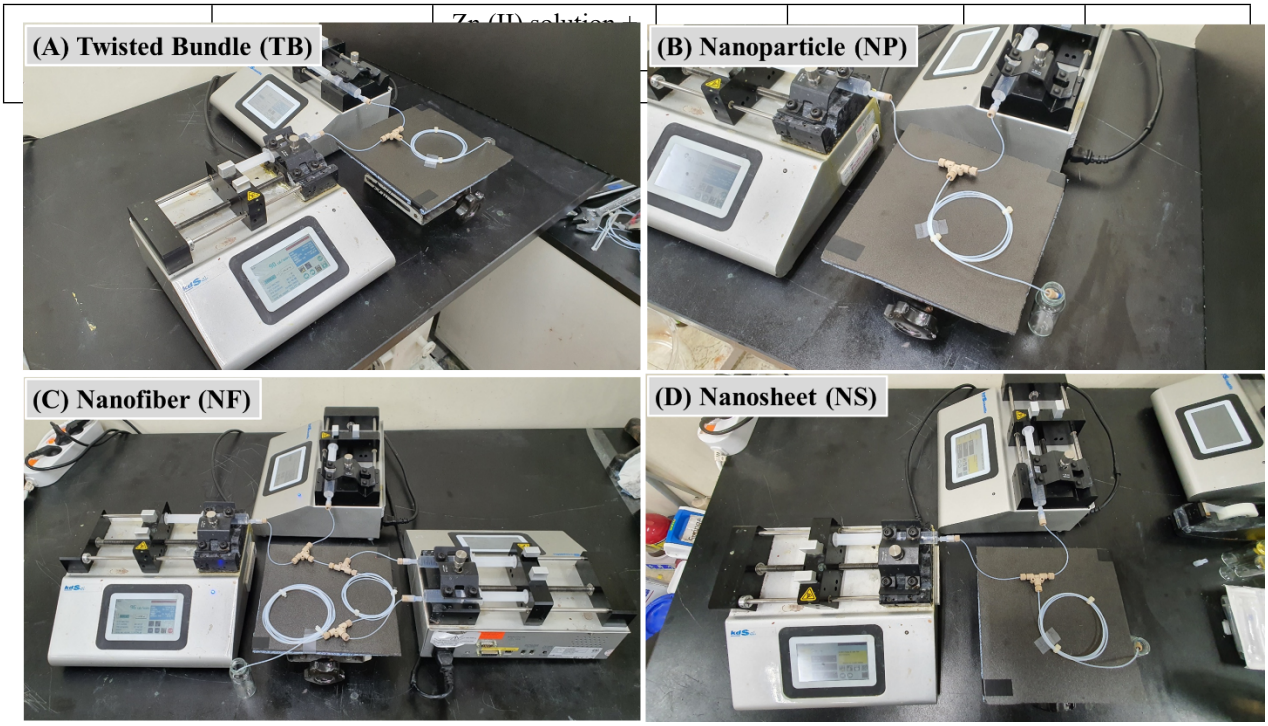

Fig. S7. Digital images of the microreactors that were used for the ultrafast self-assembly of **1** to form (A) twisted bundle (**TB**), (B) nanoparticle (**NP**), (C) Nanofiber (**NF**), and (D) Nanosheet (**NS**) at appropriate conditions.

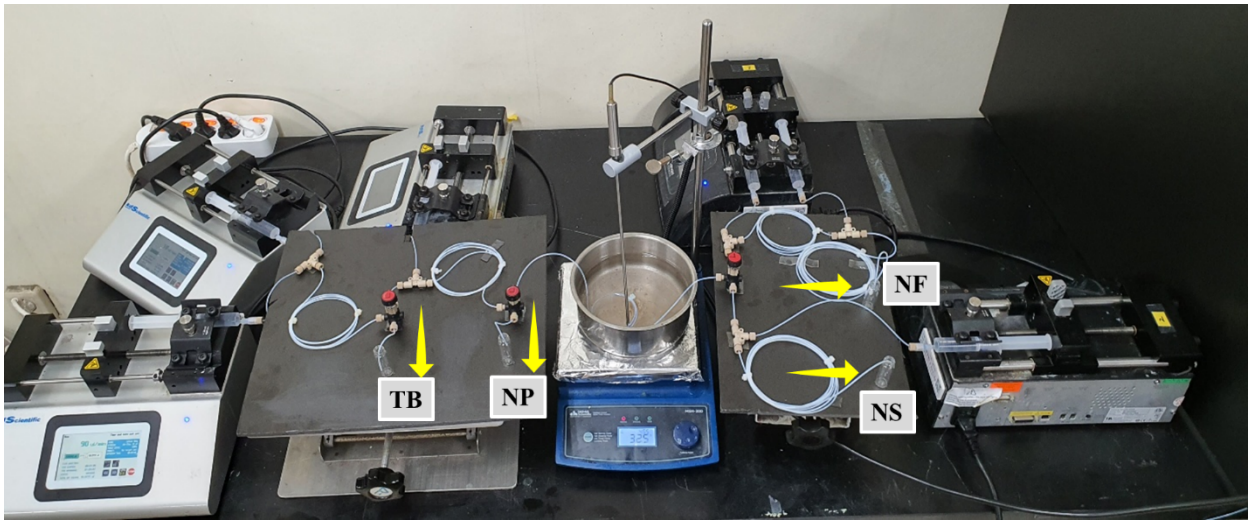

Fig. S8. Digital image of an integrated one-flow miniatured microfluidic system for the (1) ultrafast self-assembly to create various nanostructures according to the on-demand requirement which can be achieved with the help of rotary valve that could alter the direction of flow and (2) rapid *in-situ* nanostructural transformation from one to another.

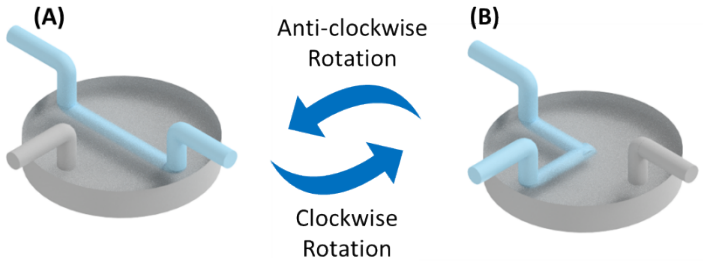

Fig. S9. Scheme showing a rotary valve (A) before and (B) after rotation that altered the flow direction and enabled to achieve on-demand nanostructure.

4. Microscopic & Spectroscopic Investigations Procedure:

Transmission Electron Microscopy (TEM): 6 µL of 0.01 mM peptide solution of **TB** was drop-casted on a 200 mesh carbon-coated copper grid. After ~5-6 minutes, the excess solution was wicked off using a whatman filter paper from entire area to have an even distribution of the self-assembly. The TEM grid was kept inside a vacuum desiccator to get dried overnight. TEM was performed using JEOL JEM 2100 with a Tungsten filament at an accelerating voltage of 200 kV. Similarly, samples for nanoparticles (**NP**), nanofibers (**NF**), and nanosheets (**NS**) were prepared following the above mentioned protocol for **TB**. A fresh aqueous uranyl acetate solution (1.2 w/v%) was used for staining the samples.

Atomic Force Microscopy: 8 µL of 0.5 mM of the **TB** solution was drop-casted on a silicon wafer. After ~15 minutes, the silicon wafer was washed by HPLC water (200-300 uL) using a micropipette to remove excess peptide solution. Subsequently, the silicon wafer was then dried using nitrogen gas blower. AFM height imaging was recorded using tapping mode tips on a Brucker and XEI 100 nanoscope. The scanned images were analyzed using NanoScope Analysis 1.5 software. The typical scan rates were selected in a range of 0.6-0.8 Hz. Following the similar procedure, samples for **NP**, **NF**, and **NS** were also prepared at similar concentration except 1 mM for nanosheets.

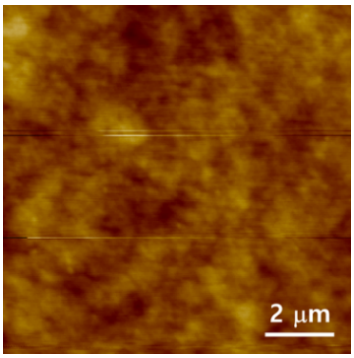

Fig. S10. AFM image showing no self-assembled structure observed when **1** was dissolved in HFIP (50 mM) to erase the presence of any pre-assembled history while synthesis and purification of **1**.

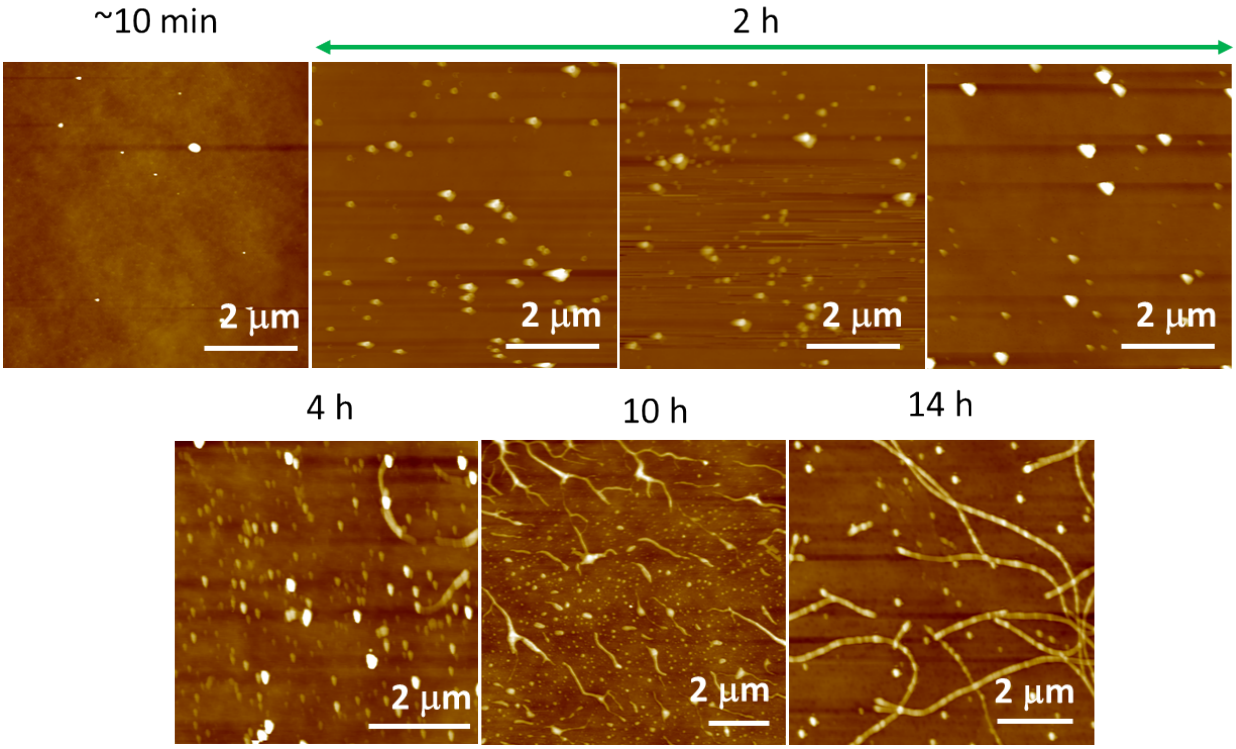

Fig. S11. AFM images demonstrating the temporal kinetics for the formation of self-assembled **TB** in 10/90% (v/v) HFIP/water at a final concentration of 5 mM at ~pH ~2-3, 25°C.

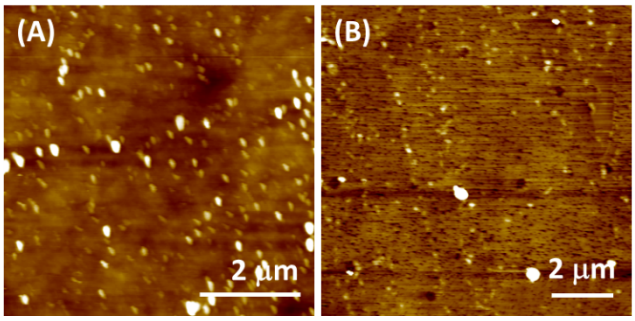

Fig. S12. AFM images recorded providing the diameter comparison of **NP** formed as a result of (A) Batch (~220 nm) and (B) Flow (~80 nm), which were stable even after 1 day at pH ~7.4-8, 25°C.

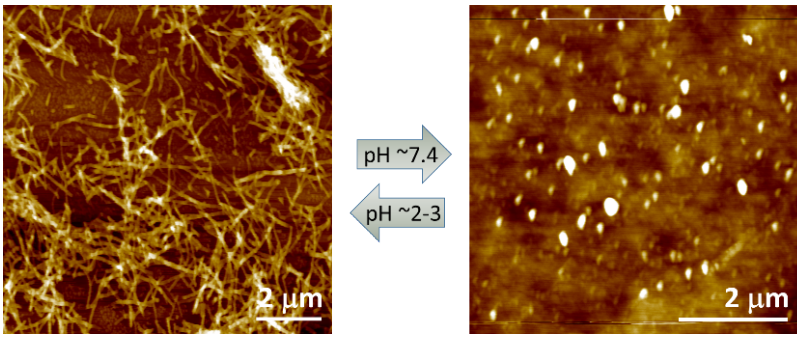

Fig. S13. AFM images show the reversibility of the **TB** to **NP** and vice versa on switching the pH values after 24 h at 25 °C.

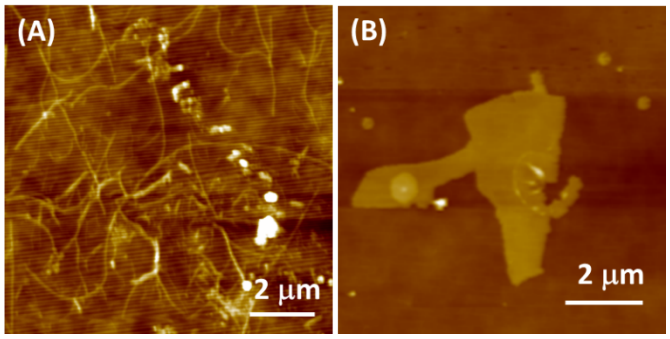

Fig. S14. AFM micrographs showing (A) **NF** and (B) **NS** as a result of the batch sample after 2 h (subsequent to oxidation) and 2 days incubation, respectively.

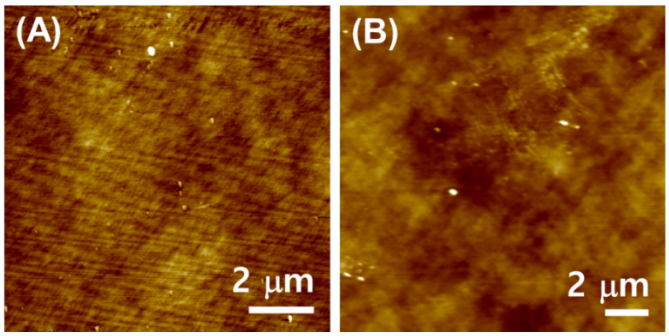

Fig. S15. AFM micrographs showing that nanostructures dis-assembles at an elevated temperature (≥55° C) as shown by AFM images where (A) Twisted Bundles, **TB**, (B) Nanofibers, **NF**. Nanostructures were stable at ambient temperature (25° C). This pinpoints the importance of non-covalent interactions among the di-peptide molecules which varies as a result of stimuli such as pH, temperature, metal etc.

Small Angle X-ray Scattering (SAXS):

The self-assembled **TB**, **NP**, **NF**, and **NS** solutions were prepared at a final concentration of 10 mM. SAXS of these various nanostructures were recorded using a line collimation system equipped with Copper source and 2-D detector and scattering patterns were fitted in different models using SASfit software using below mentioned equations:

Equation for Long Cylinder

$$\emptyset_{long}(q,R,L) = (\Delta\eta\pi R^2 L)^2 \frac{2}{QL} \times \left\{ Si\frac{\pi}{2}(QL)\Lambda_1^2(QR) - \frac{\omega(2QR)}{QL} - \frac{\sin(QL)}{(QL)^2} \right\}$$

R= Radius of the cylinder, L= Length of cylinder, Δη = scattering contrast

Equation for sphere

$$K(Q,R,\Delta\eta) = \frac{4}{3}\pi R^3 \Delta\eta \, 3 \frac{\sin QR - QR\cos QR}{(QR)^3}$$

Equation for planer object

$$P_{cs}(Q,\eta,L) = \left(\eta L \frac{\sin(QL/2)}{QL/2}\right)2$$

UV-Vis Spectrophotometer: The UV-vis spectrums were recorded using NanoDrop 2000c model spectrophotometer. To record the spectra, 0.5 mL of the peptide nanostructures solutions (0.3 mM) were added to a 10 mm path length quartz cuvette with a wide wavelength range selected from 360 nm to 190 nm.

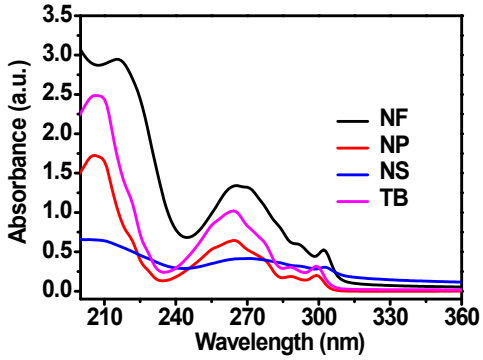

Fig. S16. UV-vis spectra of different nanostructures solutions [c=0.3 mM] were recorded at 25 °C. A similar kind of major peaks at 215 nm, 263 nm, and 295 nm were observed for **TB**, **NP**, **NF**, and **NS**.

Ellman's Test: This test is to confirm the presence free thiol groups in the reagent solution. The free thiol (SH) groups react with Ellman's reagent, cleaving the disulfide bond to give 2-nitro-5-thiobenzoate (TNB^-), which ionizes to the TNB^{2-} dianion in water at neutral and alkaline pH. This TNB^{2-} ion has a yellow color with λ_{max} = 410 nm.

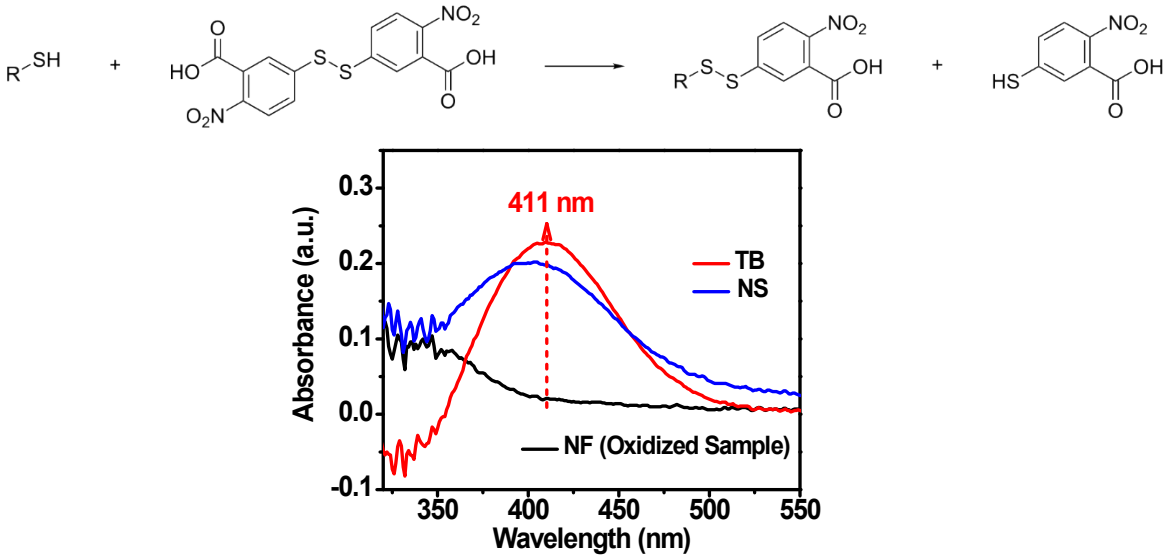

Fig. S17. UV-vis spectra of different nanostructures solutions [c=0.1 mM] were recorded at 25 °C with the addition of DTNB solution [c=0.15 mM]. No free -SH group of cysteine in an oxidized sample was observed for **NF** (**ox-1**).

Circular Dichroism (CD) Spectroscopy:

CD spectra of the peptide nanostructures to investigate the secondary structures were recorded using JASCO model J-810 Circular Dichroism Spectrophotometer. 300 µL of 0.3 mM peptide solutions were added to 2 mm path length quartz cuvette. To record the spectrum, the wavelength regime was selected from 400 nm to 190 nm with a maintained scanning speed of 100 nm/min. Three consecutive scans were accumulated to achieve a resultant final spectra.

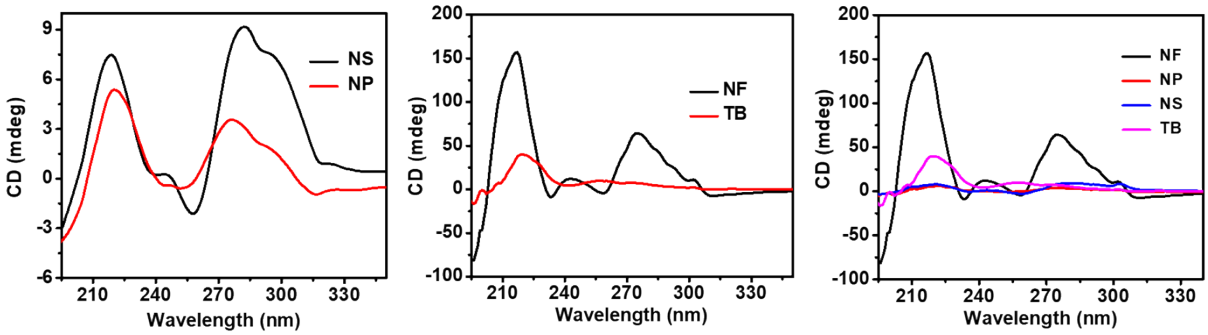

Fig. S18. A comparison of the CD spectra of different nanostructure solutions [c=0.3 mM], recorded at 25 °C. To gain insight into secondary structural estimation by the spectral manager software, it was observed that twisted bundle (**TB**) with a negative peak at 197 nm, and major positive peak at 219 nm and 262 nm showed 44.9 % turn and 55.1 % of random coil. Nanoparticle (**NP**) with a negative peak at 195 nm and positive peak at 216 nm and 274 nm inferred 41.1 % turn and 58.9 % of random coil, nanofiber (**NF**) with a negative peak 194 nm and positive peaks at 216 nm and 274 nm showed 41.6 % turn and 58.4 % of random coil, and nanosheet (**NS**) sample with a negative peak at 196 nm and major positive peaks at 221 nm and 275 nm showed 43.5 % turn and 53.5 % of random coil character.

Fluorescence (FL) Spectroscopy:

FL emission spectra of the **TB**, **NP**, **NF**, and **NS** solutions were recorded at a final concentration of 1 mM using JASCO FP-6500 WRE spectrophotometer at a fixed excitation wavelength of 280 nm corresponding

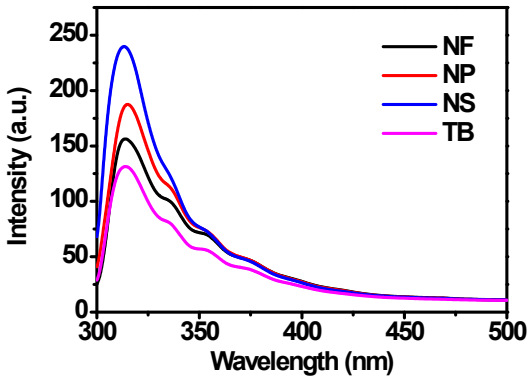

Fig. S19. A comparison of the FL emission spectra was recorded for different morphologies at 1 mM, 25° C.

to Fmoc-residue with a fixed emission spectra ranging from 300 nm to 500 nm. The fluorescence emission spectral intensity of Fmoc-residue is different for different morphology. In our case, **NS** has the maximum emission intensity whereas least for **TB** for Fmoc- with maxima emission peak at ~313 nm. The reason of a lowest emission intensity in **TB** might be attributed to the buried or closely packed Fmoc-groups, varied depending on the molecules interactions.

5. Concentrating Nanostructures Sample:

The self-assembled **TB**, **NP**, **NF**, and **NS** solutions collected using one-flow mediated miniature microfluidic reactor were concentrated to make a stock solution of higher concentration. The solutions were centrifuged at 13000 rpm for 20 min. The supernatant solution was discard followed by the addition of HPLC water and diluted solution of acetic acid for **TB** and diluted solution of NaOH for **NP**, **NF**, and **NS** with a final peptide concentration of 20 mM.

6. Rheological Characterizations:

Rheological studies for **TB** hydrogel (20 mM, 1 w/v%) were performed using Discovery HR 20 rheometer using CP 20 mm geometry. The dynamic amplitude studies were performed at a fixed angular frequency of 10 rad/s over an oscillation strain range of 0.1-100 % whereas dynamic frequency sweep mode was performed at a fixed oscillation strain value of 0.1% with a ramp of angular frequency from 0.1 to 200 rad/s. Thixotropic study was also monitored using an alternate strain value of 0.1% and 100% for 5 cycles at a fixed angular frequency (10 rad/s). All above studies were performed at 25 °C.

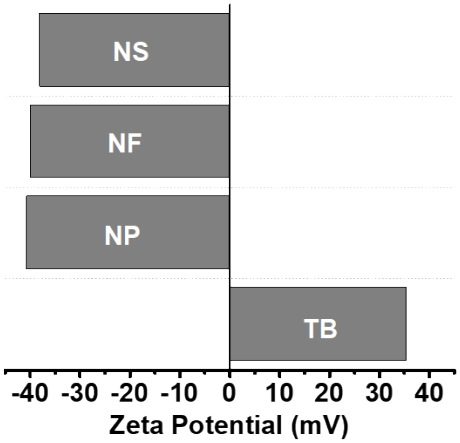

Fig. S20. A comparison of zeta potential values demonstrated the cationic nature of **TB** and anionic nature of **NP**, **NF**, and **NS**.

7. Kinetic Assays of *para*-nitrophenyl acetate (*p*-NPA) Hydrolysis:

To investigate the catalytic nature of the self-assembled nanostructures, a stock solution of *p*-NPA (100 mM) was prepared in acetonitrile (ACN). 10 µL of the stock was added to a quartz cuvette containing **NP** solution (0.1 mM, 1 mL) in 10 mM HEPES buffer, pH 7.4 at 25 °C. The kinetics spectra was recorded at a fixed wavelength of 400 nm. An increase in the absorbance value at 400 nm with the course of time confirmed the formation of a yellow coloured product, *p*-nitrophenol (*p*-NP). Various substrate concentrations were added separately to self-assembled solutions to envisage kinetics of hydrolysis and its dependency of the *p*-NPA added. Following a similar procedure, solutions of **TB**, **NF**, and **NS** were used to test the catalytic nature and their efficacy. Further, the slope values calculated from different substrate kinetics were utilized against respective concentrations for the calculation of kinetic parameters such as k_{cat}, K_M, and k_{cat}/K_M by fitting to Michaelis-Menten's equation. Following the mentioned protocol,[1,2] the performance of the nanostructures as a result of ultrafast flow process and batch process were compared.

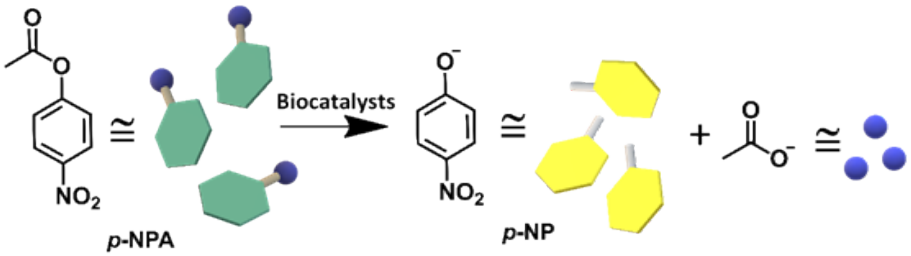

Fig. S21. A standard model reaction for the conversion of *p*-NPA to *p*-NP in the presence of nanostructures as biocatalysts.

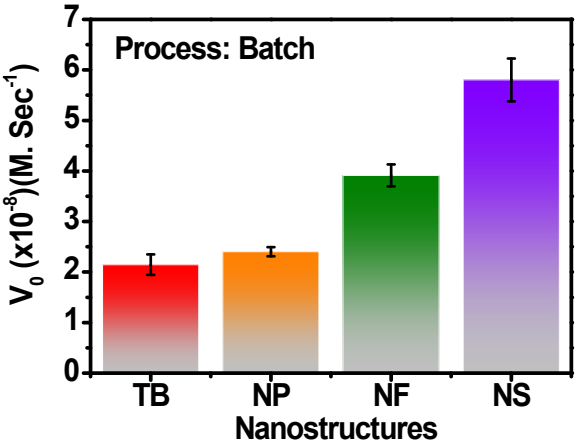

Fig. S22. Slope values for the formation of *p*-NP (0.3 mM) against **TB**, **NP**, **NF**, and **NS** (0.1 mM) self-assembled in the batch.

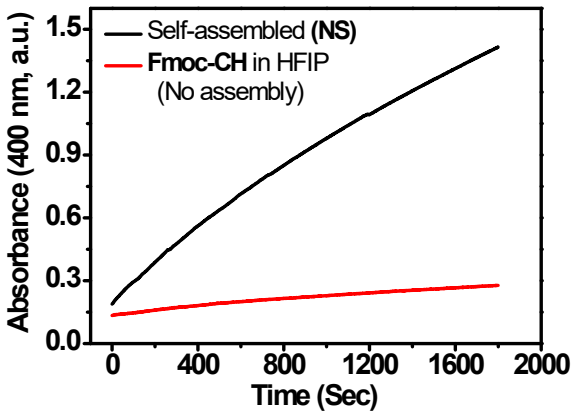

Fig. S23. Self-assembly is quite important to possess the catalytic nature. It was observed that when the **Fmoc-CH** was in the dis-assembled state (HFIP), it does not show any catalytic behavior as compared to the self-assembled nanosheet (**NS**). The reason could be attributed to the generation of hydrolase mimicked active site as a result of self-assembly where the histidine residues on the active site take part in catalyzing the incoming substrate *p*-NPA and thereby result in the formation of *p*-NP.

References:

1 A. Singh, J. P. Joseph, D. Gupta, C. Miglani, N. A. Mavlankar and A. Pal, *Nanoscale*, 2021, **13**, 13401–13409.

2 Z. Lengyel, C. M. Rufo, Y. S. Moroz, O. V. Makhlynets and I. V. Korendovych, *ACS Catal.*, 2018, **8**, 59–62.